# Cyclicity of degenerate graphic DF2a of Dumortier-Roussarie-Rousseau program

Peer-reviewed author version

HUZAK, Renato (2018) Cyclicity of degenerate graphic DF2a of Dumortier-Roussarie-Rousseau program. In: COMMUNICATIONS ON PURE AND APPLIED ANALYSIS, 17(3), p. 1305-1316.

DOI: 10.3934/cpaa.2018063
Handle: http://hdl.handle.net/1942/25661

COMMUNICATIONS ON
PURE AND APPLIED ANALYSIS
Volume , Number **0**,

doi:

pp. **000–000**

# CYCLICITY OF DEGENERATE GRAPHIC $DF_{2a}$ OF DUMORTIER-ROUSSARIE-ROUSSEAU PROGRAM

Renato Huzak

Hasselt University, Campus Diepenbeek, Agoralaan Gebouw D
3590 Diepenbeek, Belgium

Abstract. In this paper we finish the study of the cyclicity ( i.e. the maximum number of limit cycles) of the degenerate graphic $DF_{2a}$ of [6] which is initiated in [5]. More precisely, we prove that the graphic $DF_{2a}$ has a finite cyclicity. The goal of the program [6] is to solve the finiteness part of Hilbert's 16th problem for quadratic polynomial systems. We use techniques from geometric singular perturbation theory, including the family blow-up.

1. **Introduction.** The second part of the famous Hilbert's 16th problem is formulated in the following way: *determine the maximum number $H(n)$ and the relative positions of limit cycles of a planar polynomial vector field if the polynomial degree $n$ of the vector field is given.* See [9]. This problem is more than 100 years old and still open even in the case of quadratic polynomial vector fields ($n = 2$). To prove the uniform finiteness for the quadratic vector fields, i.e., $H(2) < \infty$, F. Dumortier, R. Roussarie & C. Rousseau formulated a program (see [6]) consisting of 121 local finiteness problems. Slightly more precisely, the DRR program reduces the proof that $H(2) < \infty$ to the proof that 121 graphics inside quadratic systems have a finite cyclicity. We refer to [8] for an overview of the graphics whose finite cyclicity is proved at the time.

Some of these graphics are *degenerate*, having a line of singular points in the finite plane or at infinity. There are 13 such graphics and the systematic study of their cyclicity began with [5], using geometric singular perturbation theory (GSPT) and the family blow-up applied to GSPT (see e.g. [4]). The paper [5] more specifically deals with the study of the cyclicity of the degenerate graphics $DF_{1a}$ and $DF_{2a}$ of the DRR program, having a line of singularities in the finite plane. We consider quadratic systems $X_{\epsilon,b,(D,E_0,E_1,E_2)}$ where $X_{\epsilon,b,(D,E_0,E_1,E_2)}$ stands for (see [5])

$$\begin{cases} \dot{x} = y + bxy - y^2 + \epsilon^2(E_0 + E_1x + E_2x^2) \\ \dot{y} = xy + \epsilon^3 D \end{cases} \tag{1}$$

with $\epsilon \geq 0$ small, $b \in [0, 2[$ and $(D, E_0, E_1, E_2) \in \mathcal{C}$. The set $\mathcal{C}$ is the boundary of a cylinder:

$$\mathcal{C} = \mathcal{B}_0 \cup \mathcal{B}_+ \cup \mathcal{B}_-$$

where

$$\mathcal{B}_0 = \{(D, E_0, E_1, E_2) \in \mathbb{R}^4 \ \mid D \in [-1, 1], (E_0, E_1, E_2) \in \mathbb{S}^2\}$$

and

$$\mathcal{B}_\pm = \{(D, E_0, E_1, E_2) \in \mathbb{R}^4 \ \mid D = \pm 1, E_0^2 + E_1^2 + E_2^2 \leq 1\}.$$

When $\epsilon = 0$, the system (1) has the line of singular points $\{y = 0\}$. The set $\{y = 0\}$ is called the critical curve. All these singular points are semi-hyperbolic, except for the origin $(x, y) = (0, 0)$, where we have a nilpotent contact point. (For more details on definitions of the critical curve, semi-hyperbolic singularities, nilpotent contact points etc., see e.g. [1].) The degenerate graphic $DF_{1a}$ (resp. $DF_{2a}$) is observed in the fast subsystem $X_{0,b,(D,E_0,E_1,E_2)}$, for $b \in ]0, 2[$ (resp. $b = 0$). See Figure 1. The degenerate graphics $DF_{1a}$ and $DF_{2a}$ consist of an orbit of the fast subsystem $X_{0,b,(D,E_0,E_1,E_2)}$ and the part of the critical curve between the $\alpha$-limit $(x_*, 0)$, $x_* > 0$, and the $\omega$-limit $(F_b(x_*), 0)$ of that orbit (see Figure 1).

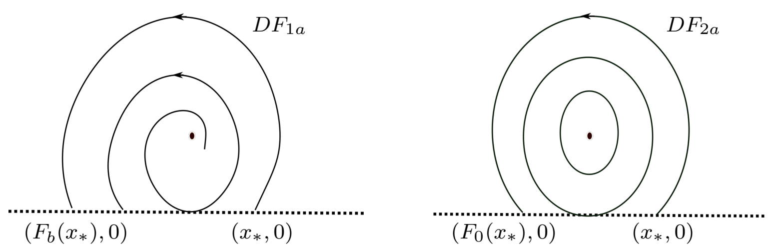


FIGURE 1. The degenerate graphics $DF_{1a}$ ($b \in ]0, 2[$) and $DF_{2a}$ ($b = 0$).

**Remark 1.** Let's explain where (1) comes from. By Proposition 2.1 of [5], a quadratic system with a line of singularities in the finite plane (all the singularities except one are normally hyperbolic) and a focus (strong or weak) or center can be brought to the form $Q : \{\dot{x} = y + b_0xy - y^2, \dot{y} = xy\}$, where $b_0 \in ] - 2, 2[$. There are 6 graphics with a line of singular points in the finite plane: $DF_{1a}$, $DF_{1b}$, $DF_{2a}$, $DF_{2b}$, $DH_1$ and $DH_2$ (see [5] or Figure 11 of [6]). Moreover, Proposition 2.1 of [5] implies that the general quadratic perturbation of $Q$ has the following form, after an affine change of coordinates and time scaling: $\{\dot{x} = y + bxy - y^2 + \mu_1 + \mu_2x + \mu_3x^2, \dot{y} = xy + \mu_4\}$, where $b = b_0 + \mu_0 \in [0, 2[$. When we deal with $DF_{1a}$ and $DF_{2a}$, it is more convenient to write $(\mu_1, \mu_2, \mu_3, \mu_4) = (\epsilon^2E_0, \epsilon^2E_1, \epsilon^2E_2, \epsilon^3D)$, with $(D, E_0, E_1, E_2) \in \mathcal{C}$ (for more details see [5]). This gives (1).

The degenerate graphics $DF_{1a}$ and $DF_{2a}$ can generate limit cycles in the systems (1), with $\epsilon > 0$. Their cyclicity has been studied in [5] in the case $(D, E_0, E_1, E_2) \neq P_0 := (0, 0, 0, 1)$, $(D, E_0, E_1, E_2) \in \mathcal{C}$. Under this condition on $(D, E_0, E_1, E_2)$, one deals with a slow dynamics along the critical curve with non-zero isolated singularities on $[F_b(x_*), x_*]$, and the results presented in [1] and [2] can be used to study the cyclicity of $DF_{1a}$ and $DF_{2a}$. We refer to [5] for more details. However, in [5] it was not possible to study the cyclicity of $DF_{1a}$ and $DF_{2a}$ in slow-fast systems

$$\begin{cases} \dot{x} = y + bxy - y^2 + \epsilon^2(e_0 + e_1x + x^2) \\ \dot{y} = xy + \epsilon^3D, \end{cases} \tag{2}$$

with $(D, e_0, e_1) \sim (0, 0, 0)$, $\epsilon \sim 0$ and $b \in [0, 2[$, because a singularity of the slow dynamics $x' = e_0 + e_1x + x^2$ of (2) can be located at the contact point $x = 0$. Note that the system (2) represents (1) with $(D, E_0, E_1, E_2) \sim P_0$ and $(D, E_0, E_1, E_2) \in \mathcal{C}$. In fact, instead of using the spherical coordinates near $P_0$, it is more convenient to work in the chart $(D, E_0, E_1, E_2) = (D, e_0, e_1, 1)$, $(D, e_0, e_1) \sim (0, 0, 0)$, covering $\mathcal{C}$ near $P_0$ (for more details see [5]). Since there is no difference between (1) and (2) for $\epsilon = 0$, we deal with the same degenerate graphics in the family (2), $DF_{1a}$ and $DF_{2a}$.

Later, it has been proved in [3] that the cyclicity of $DF_{1a}$ in (2) is finite. The paper [3] treats the cyclicity of so-called detectable canard cycles by studying zeros of the derivative of the related slow divergence integral if the slow dynamics is regular, except for the contact point, where a saddle-node singularity occurs. *The case $DF_{2a}$ ($b = 0$) is technically far more difficult due to the center problem and our goal is to study this case using techniques from singular perturbation theory and the family blow-up developed in [3] and [7].*

Denote the degenerate graphic $DF_{2a}$ by $\Gamma_{x_*}$, where $x_* \in K$, with $K \subset ]0, \infty[$ compact. In Section 2 we prove

**Theorem 1.1.** *There exist small $\epsilon_0 > 0$, $b_0 > 0$, $d > 0$ and a $(D, e_0, e_1)$-neighborhood $W$ of the origin such that system (2) has at most three limit cycles (counting multiplicity) within Hausdorff distance $d$ of $\Gamma_{x_*}$, for each value $(x_*, \epsilon, b, D, e_0, e_1) \in K \times [0, \epsilon_0] \times [-b_0, b_0] \times W$.*

**Remark 2.** It will be clear from the proof of Theorem 1.1 (see Section 2) that the cyclicity of $\cup_{x_* \in K} \Gamma_{x_*}$ is bounded by 3. In this paper we don't study the cyclicity of the limit periodic sets $\Gamma_0$ and $\Gamma_\infty$, denoted by $DF_{2b}$ and $DH_2$ in [6]. As far as we know, these two cases are open (see [8, 5]) and different techniques are needed to treat them. The same is true for the two limiting cases ($DF_{1b}$ and $DH_1$) for $b > 0$.

Combining Theorem 1.1, Theorem 3.1 of [5] and Theorem 7 of [3], we obtain a cyclicity result for the complete unfolding (1):

**Theorem 1.2.** *Consider a system $X_{\epsilon,b,(D,E_0,E_1,E_2)}$ given in (1) and a family of degenerate graphics $\Gamma_{x_*}^{b_*}$, where $\epsilon \geq 0$ small, $b_* \in [0, 2[$, $(D, E_0, E_1, E_2) \in \mathcal{C}$ and $x_* \in K$, with $K \subset ]0, \infty[$ compact (the degenerate graphics $\Gamma_{x_*}^{b_*}$ are of type $DF_{1a}$ for $b_* \in ]0, 2[$ and the degenerate graphics $\Gamma_{x_*}^{0}$ are of type $DF_{2a}$). Then the following statements are true:*

- *(i)* ***(finite cyclicity of** $DF_{1a}$**)** If $b_* \in ]0, 2[$, there exist $\epsilon_0 > 0$, $\eta_0 > 0$ and $\rho_0 > 0$ such that system (1) with $\epsilon \in [0, \epsilon_0]$ and $b \in [b_* - \eta_0, b_* + \eta_0]$ has at most three limit cycles (multiplicity taken into account), lying each within Hausdorff distance $\rho_0$ of a corresponding slow-fast cycle $\Gamma_{x_*}^{b_*}$, with $x_* \in K$. If moreover we keep $E_1 \geq 0$, then, under the same conditions on $(\epsilon, b)$, system (1) has at most one limit cycle, which is hyperbolic and attracting when it exists.*
- *(ii)* ***(finite cyclicity of** $DF_{2a}$**)** If $b_* = 0$, there exist $\epsilon_0 > 0$, $\eta_0 > 0$ and $\rho_0 > 0$ such that system (1) with $\epsilon \in [0, \epsilon_0]$ and $b \in [-\eta_0, \eta_0]$ has at most five limit cycles (multiplicity taken into account), lying each within Hausdorff distance $\rho_0$ of a corresponding slow-fast cycle $\Gamma_{x_*}^{0}$, with $x_* \in K$.*
- *(iii) Let $B_\delta(P_0)$ (resp. $B_{\delta_1}((0, E_0, 0, E_2))$) be a $\delta$-neighbourhood (resp. a $\delta_1$-neighbourhood) of $P_0 = (0, 0, 0, 1)$ (resp. the circle $\{D = E_1 = 0\}$) inside $\mathcal{C}$. If $b_* = 0$ and $\delta$ and $\delta_1$ are arbitrary, then there exist $\epsilon_0 > 0$ and $\eta_0 > 0$ such that the system (1) with $\epsilon \in [0, \epsilon_0]$, $b \in [-\eta_0, \eta_0]$ and $(D, E_0, E_1, E_2) \in \mathcal{C} \setminus (B_\delta(P_0) \cup B_{\delta_1}((0, E_0, 0, E_2)))$ has at most one limit cycle and this limit cycle is hyperbolic; it is repelling for $E_1 < 0$ and attracting for $E_1 > 0$.*

**Remark 3.** Theorem 1.2(i) follows directly from Theorem 3.1(i) of [5] (the parameter $(D, E_0, E_1, E_2) \neq P_0$) and Section 4.2 of [3] ($(D, E_0, E_1, E_2) \sim P_0$). On the other hand, Theorem 1.1 ($(D, E_0, E_1, E_2) \sim P_0$) and Theorem 3.1(ii) of [5] ($(D, E_0, E_1, E_2) \neq P_0$) imply Theorem 1.2(ii). Statement (iii) of Theorem 1.2 has been proved in [5], Theorem 3.1(iii).

## 2. **Proof of Theorem 1.1.**

2.1. **Slow dynamics and slow divergence integral.** In this section we focus on systems (2), where $\epsilon \geq 0$ is small and $(b, D, e_0, e_1) \sim (0, 0, 0, 0)$. We denote (2) by $X_{\epsilon,b,(D,e_0,e_1)}$. The slow dynamics is given by

$$x' = e_0 + e_1 x + x^2, \ x \neq 0.$$

When limit cycles are Hausdorff-close to $\Gamma_{x_*}$, the slow dynamics allows the passage from the attracting part of the critical curve to the repelling part of the critical curve, for some parameters $(e_0, e_1)$. Note that the slow dynamics is strictly positive for $(e_0, e_1) = (0, 0)$, except for the origin $x = 0$, where it has a saddle-node singularity. See Figure 2. The passage near the saddle-node singularity has to be studied separately from the rest of the critical curve using blow-up techniques from [3] or [7]. It will be explained later in this section.

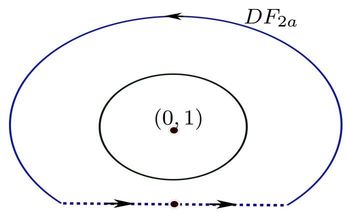


FIGURE 2. The degenerate graphic $DF_{2a}$ and the indication of the slow dynamics of (2) for $e_0 = e_1 = 0$. One can expect limit cycles of (2) to bifurcate from $DF_{2a}$.

Following [3], an upper bound for the number of limit cycles near the set $\cup_{x_* \in K} \Gamma_{x_*}$, with $K \subset ]0, \infty[$ compact, could be found by studying zeros of the derivative $\frac{\partial I}{\partial x_*}$ of the slow divergence integral with respect to $x_*$ along $[F_b(x_*), x_*]$

$$I(x_*, b, e_0, e_1) = \int_{F_b(x_*)}^{x_*} \frac{x dx}{e_0 + e_1 x + x^2},$$

with $(b, e_0, e_1) \sim (0, 0, 0)$, $x_* \in K$ and with $F_b(x_*)$ defined in Section 1. Clearly, the divergence of $X_{0,b,(D,e_0,e_1)}$ on the critical curve $\{y = 0\}$ is $x$ and $dt = \frac{dx}{e_0 + e_1 x + x^2}$. Although the slow divergence integral $I$ is divergent for $e_0 = e_1 = 0$, its derivative w.r.t. $x_*$

$$\frac{\partial I}{\partial x_*}(x_*, b, e_0, e_1) = \frac{x_*}{e_0 + e_1 x_* + x_*^2} - \frac{F_b(x_*) \frac{\partial F_b}{\partial x_*}(x_*)}{e_0 + e_1 F_b(x_*) + F_b(x_*)^2} \tag{3}$$

is well defined for $x_* \in K$ and $(e_0, e_1) \sim (0, 0)$. When $b > 0$, (3) is nonzero for $(e_0, e_1) = (0, 0)$ (see [3]) and it helps us find the number of zeros of the derivative of the "full" divergence integral of (2) which is related to the cyclicity of $DF_{1a}$ in the family (2) (see Theorem 5 of [3]).

Note that $F_b(x_*) = -x_* + O(b)$ because the system $X_{0,0,(D,e_0,e_1)}$ is invariant under $(x, t) \mapsto (-x, -t)$ with a center at $(x, y) = (0, 1)$. Thus, $\frac{\partial I}{\partial x_*}(x_*, b, e_0, e_1)$ is identically zero for $b = e_1 = 0$, and this degenerate case cannot be studied using

Theorem 5 of [3]. In order to prove Theorem 1.1, we have to improve some results given in [3] by studying the derivative of the full divergence integral of $X_{\epsilon,b,(D,e_0,e_1)}$ and using symmetries of $X_{\epsilon,b,(D,e_0,e_1)}$.

2.2. **Normal form near the contact point and reduction to slow-fast Hopf parameter regions.** To find the regions in the parameter space $(D, e_0, e_1)$ where the passage near the contact point at the origin $(x, y) = (0, 0)$ is possible, we first blow up the origin $(D, e_0, e_1) = (0, 0, 0)$ using a quasi-homogeneous blow-up

$$(D, e_0, e_1) = (r^3\tilde{D}, r^2\tilde{e}_0, r\tilde{e}_1),\ (\tilde{D}, \tilde{e}_0, \tilde{e}_1) \in \mathbb{S}^2,\ r \geq 0,\ r \sim 0.$$

After this blow-up in the $(D, e_0, e_1)$-space, the slow-fast system (2) becomes

$$\begin{cases} \dot{x} = y + bxy - y^2 + \epsilon^2(r^2\tilde{e}_0 + r\tilde{e}_1 x + x^2) \\ \dot{y} = xy + \epsilon^3 r^3\tilde{D}. \end{cases} \tag{4}$$

Clearly, instead of studying systems (2), with $(D, e_0, e_1)$ in a small neighborhood of the origin $(D, e_0, e_1) = (0, 0, 0)$, it suffices to study systems (4), with $r \sim 0$ and with $(\tilde{D}, \tilde{e}_0, \tilde{e}_1)$ on a 2-dimensional sphere. In order to desingularize systems (4), we can combine two blow-up constructions (see [3] or [7]): *a primary blow-up* $(x, y, r) = (u\bar{x}, u^2\bar{y}, u\bar{r})$, $(\bar{x}, \bar{y}, \bar{r}) \in \mathbb{S}^2$, $\bar{r} \geq 0$, where we blow up the phase coordinates $(x, y)$ and the parameter $r \geq 0$, and a *secondary blow-up* $(\bar{x}, \bar{y}, \epsilon) = (\delta\tilde{x}, \delta^2\tilde{y}, \delta\tilde{\epsilon})$, $(\tilde{x}, \tilde{y}, \tilde{\epsilon}) \in \mathbb{S}^2$, $\tilde{\epsilon} \geq 0$, where the new phase coordinates $(\bar{x}, \bar{y})$ and the singular perturbation parameter $\epsilon \geq 0$ are included in the blow-up. Rather than repeating the calculations from [3] for slow-fast systems (4) near the contact point in different charts of the primary and secondary blow-up, we bring (4) near the contact point to a normal form studied in [3], and we use the results from [3] directly. Using the coordinate change

$$Y = y + bxy - y^2 \ \left(i.e.,\ y = Y\big(1 - bx + O(Y) + O(x^2)\big)\right)$$

near $(x, y) = (0, 0)$, (4) becomes

$$\begin{cases} \dot{x} = Y + \epsilon^2(e_0 + e_1 x + x^2) \\ \dot{Y} = \epsilon^3 D(1 + bx) + Y\big(\epsilon^2\alpha_1 + (1 + \epsilon^2\alpha_2)x + O(x^2)\big) + O(Y^2), \end{cases} \tag{5}$$

where $(D, e_0, e_1) = (r^3\tilde{D}, r^2\tilde{e}_0, r\tilde{e}_1)$, $\alpha_1 = be_0 - 2\epsilon D$ and $\alpha_2 = -b^2 e_0 + be_1 + 2b\epsilon D$. After the change of coordinates $\bar{Y} = -\big(Y + \epsilon^2(e_0 + e_1 x + x^2)\big)$, and after division by $-1$, systems (5) change into

$$\begin{cases} \dot{x} = \bar{Y} \\ \dot{\bar{Y}} = \epsilon^2\big(\epsilon b_0 + b_1 x + b_2 x^2 + b_3 x^3 + O(x^4)\big) \\ \qquad + \big(\epsilon^2 O(D, e_0, e_1) + (-1 + O(\epsilon))x + O(x^2)\big)\bar{Y} + O(\bar{Y}^2), \end{cases} \tag{6}$$

where $b_0 = D + \epsilon O(De_0, e_0^2)$, $b_1 = -e_0 + \epsilon O(D, e_0^2, e_0 e_1)$, $b_2 = -e_1 + O(D, e_0, e_1^2)$ and $b_3 = -1 + O(D, e_0, e_1)$. After a translation $\bar{X} = x - O(\epsilon^2 D, \epsilon^2 e_0, \epsilon^2 e_1)$ we may (and will) assume that $\epsilon^2 O(D, e_0, e_1) = 0$ in (6), and after a rescaling of $(\bar{X}, \bar{Y}, t)$ we have $-1 + O(\epsilon) = -1$ in (6). More precisely, (6) changes into

$$\begin{cases} \dot{\bar{X}} = \bar{Y} \\ \dot{\bar{Y}} = -\bar{X}\bar{Y} + \epsilon^2\big(\epsilon b_0 + b_1\bar{X} + b_2\bar{X}^2 + b_3\bar{X}^3 + O(\bar{X}^4)\big) + O(\bar{X}^2\bar{Y}, \bar{Y}^2) \end{cases} \tag{7}$$

with $b_0 = D + \epsilon O(D, e_0^2, e_0 e_1, e_1^3)$, $b_1 = -e_0 + \epsilon O(D, e_0, e_1^2)$, $b_2 = -e_1 + O(D, e_0, e_1^2, \epsilon e_1)$ and $b_3 = -1 + O(\epsilon, D, e_0, e_1)$. Systems (7) are of the form (5) of [3], implying that the results of [3] can be applied. The system (5) of [3] has the following form:

$$\begin{cases} \dot{x} = y \\ \dot{y} = -xy + \epsilon^2\big(\epsilon a_0 + a_1 x + a_2 x^2 - x^3 + G(x,y,\lambda)\big) + yH(x,y,\lambda), \end{cases}$$

where $\epsilon > 0$, $\epsilon \sim 0$, $(a_0, a_1, a_2) \sim (0,0,0)$, $\lambda$ is kept in a compact subset of $\mathbb{R}^p$, for some $p \geq 1$, $G$ and $H$ are smooth near the origin with $G = O(x^4, x^2y, y^2)$ and $H = O(x^2, y)$.

Taking into account $(D, e_0, e_1) = (r^3\tilde{D}, r^2\tilde{e}_0, r\tilde{e}_1)$, (7) can be written as

$$\begin{cases} \dot{\bar{X}} = \bar{Y} \\ \dot{\bar{Y}} = -\bar{X}\bar{Y} + \epsilon^2\big(\epsilon r^3 B_0 + r^2 B_1 \bar{X} + r B_2 \bar{X}^2 - (1 + O(\epsilon, r))\bar{X}^3 + O(\bar{X}^4)\big) \\ \qquad + O(\bar{X}^2\bar{Y}, \bar{Y}^2) \end{cases} \tag{8}$$

with $B_0 = \tilde{D} + O(\epsilon)$, $B_1 = -\tilde{e}_0 + O(\epsilon)$ and $B_2 = -\tilde{e}_1 + O(\epsilon, r)$. Note that $B_0^2 + B_1^2 + B_2^2 = 1 + O(\epsilon, r)$ because $(\tilde{D}, \tilde{e}_0, \tilde{e}_1) \in \mathbb{S}^2$. In Section 3.2 of [3], instead of working with the spherical coordinates, 6 different charts (or regions) of the sphere have been used (see also [7]):

- **Jump region (JR)**
  $B_0 = \pm 1$, $(B_1, B_2) \in K_0$, where $K_0$ is a sufficiently large compact set in $\mathbb{R}^2$.
- **Saddle region (SR)**
  $B_1 = 1$, $B_0 \in U_1$, $B_2 \in K_1$, where $U_1$ is a sufficiently small neighborhood of the origin in $\mathbb{R}$ and where $K_1$ is a sufficiently large compact set in $\mathbb{R}$.
- **Slow-fast Hopf region (SFHR)**
  $B_1 = -1$, $B_0 \in U_1$, $B_2 \in K_1$, where $U_1$ is a sufficiently small neighborhood of the origin in $\mathbb{R}$ and where $K_1$ is a sufficiently large compact set in $\mathbb{R}$.
- **Slow-fast Bogdanov-Takens region (SFBTR)**
  $B_2 = \pm 1$, $(B_0, B_1) \in U_2$, where $U_2$ is a sufficiently small neighborhood of the origin in $\mathbb{R}^2$.

Clearly, for any small $U_1$ and $U_2$ we can take the compact sets $K_0$ and $K_1$ large enough such that the chosen charts cover a complete neighborhood of $(0,0,0)$ in the $(D, e_0, e_1)$-space.

By Theorem 1 of [3], the passage near the contact point of (8) from the section $\{\bar{X} = \rho\}$ to the section $\{\bar{X} = -\rho\}$ ($\rho > 0$ small) is possible only for the parameters $(B_0, B_1, B_2)$ in the slow-fast Hopf region $\{B_1 = -1\}$: $B_0 \sim 0$ and $B_2 \in [-B_2^0, B_2^0]$, with $B_2^0 > 0$ large and fixed. This, together with the fact that (5) was divided by $-1$ and $B_1 = -\tilde{e}_0 + O(\epsilon)$, implies that the passage near the contact point of (4) from $\{x = -\rho\}$ to $\{x = \rho\}$ is only possible for the parameters $(\epsilon, D, e_0, e_1) \sim (0,0,0,0)$ with the property that

$$(D, e_0, e_1) = (r^3\tilde{D}, r^2, r\tilde{e}_1), \ \epsilon > 0, \ r > 0, \ \tilde{D} \sim 0, \ \tilde{e}_1 \in [-\tilde{e}_1^0, \tilde{e}_1^0],$$

with $\tilde{e}_1^0 > 0$ large and fixed.

**Remark 4.** The canard limit cycles of (4) Hausdorff-close to $DF_{2a}$ are not possible in the charts $\{\widetilde{D} = \pm 1\}$, $\{\tilde{e}_0 = -1\}$ and $\{\tilde{e}_1 = \pm 1\}$ covering $\mathbb{S}^2 \setminus \{\tilde{e}_0 = 1\}$ in the $(\tilde{D}, \tilde{e}_0, \tilde{e}_1)$-space. Indeed, $\{\widetilde{D} = \pm 1\}$ corresponds to the jump region $\{B_0 = \pm 1\}$ ($B_0 = \widetilde{D} + O(\epsilon)$), $\{\tilde{e}_0 = -1\}$ corresponds to the saddle region $\{B_1 = 1\}$ ($B_1 = -\tilde{e}_0 + O(\epsilon)$) and $\{\tilde{e}_1 = \pm 1\}$ corresponds to the slow-fast Bogdanov-Takens region $\{B_2 = \pm 1\}$ ($B_2 = -\tilde{e}_1 + O(\epsilon, r)$). Theorem 1 of [3] implies now that the passage near the contact point of (8) (hence the passage near the contact point of (4)) is

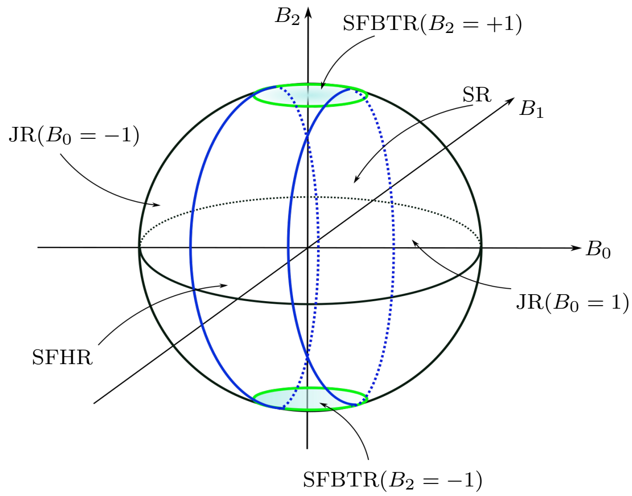


FIGURE 3. Six regions covering the sphere in the $(B_0, B_1, B_2)$-space. Canard limit cycles of (4), Hausdorff-close to $DF_{2a}$, are only possible for the parameters in the slow-fast Hopf region.

not possible in the jump, saddle and slow-fast Bogdanov-Takens regions. Thus the canard limit cycles of (4) are only possible in the chart $\{\tilde{e}_0 = 1\}$.

For the sake of completeness, we give a sketch of the proof of Theorem 1 of [3] (for more details see Sections 3.2.5-3.2.6 of [3]). After the (singular) change of coordinates $(x, y) = (r\bar{x}, r^2\bar{y})$, with $(\bar{x}, \bar{y})$ kept in a compact set, and after division by $r > 0$, (4) becomes $X_P : \{\dot{\bar{x}} = \bar{y} + br\bar{x}\bar{y} - r^2\bar{y}^2 + \epsilon^2(\tilde{e}_0 + \tilde{e}_1\bar{x} + \bar{x}^2), \dot{\bar{y}} = \bar{x}\bar{y} + \epsilon^3\tilde{D}\}$. The slow-fast vector field $X_P$ represents (4) in the family directional chart $\{\bar{r} = 1\}$ of the primary blow-up defined after (4). When $\epsilon = 0$, the vector field $X_P$ has the line of singularities $\{\bar{y} = 0\}$ that connects the attracting part and the repelling part of the critical curve $\{y = 0\}$ of (4). All the singularities are semi-hyperbolic on the critical curve $\{\bar{y} = 0\}$, except for the origin $\bar{x} = 0$, where we deal with the nilpotent contact point. The slow dynamics of $X_P$, along $\{\bar{y} = 0\}$, is given by

$$\bar{x}' = \tilde{e}_0 + \tilde{e}_1\bar{x} + \bar{x}^2.$$

First, suppose that $\tilde{e}_1 = \pm 1$ and $(\tilde{D}, \tilde{e}_0) \sim (0, 0)$. Then the slow dynamics has a hyperbolic singularity near $\bar{x} = 1$ (resp. $\bar{x} = -1$) when $\tilde{e}_1 = -1$ (resp. $\tilde{e}_1 = 1$). This implies that in this chart the slow dynamics cannot go from $\bar{x} = -\infty$ to $\bar{x} = +\infty$ (hence the passage from the attracting part to the repelling part of the critical curve of (4) is not possible). Suppose now that $\tilde{D} \sim 0$, $\tilde{e}_0 = \pm 1$ and $\tilde{e}_1$ is kept in an arbitrary compact set. When $\tilde{e}_0 = -1$, the slow dynamics is negative near $\bar{x} = 0$, and therefore it cannot go from $\bar{x} = -\infty$ to $\bar{x} = +\infty$. When $\tilde{e}_0 = 1$, the slow dynamics is (uniformly) positive for some values of the parameter $\tilde{e}_1$ (in this chart, the passage is possible). Finally, suppose that $\tilde{D} = \pm 1$, with $(\tilde{e}_0, \tilde{e}_1)$ kept in a compact set. In this chart, the slow dynamics has a saddle-node at $\bar{x} = 0$, for $(\tilde{e}_0, \tilde{e}_1) = (0, 0)$, like the (original) slow dynamics of (4). In this chart, we use the secondary blow-up, defined after (4), to show that the origin $(\bar{x}, \bar{y}) = (0, 0)$ is a jump point (see Section 3.2.6 of [3]). In the family chart $\{\tilde{\epsilon} = 1\}$, the secondary blow-up formula becomes $(\bar{x}, \bar{y}) = (\epsilon\tilde{x}, \epsilon^2\tilde{y})$, with $(\tilde{x}, \tilde{y})$ kept in a compact set. After this rescaling and division by $\epsilon > 0$, $X_P$ changes to $X_S : \{\dot{\tilde{x}} = \tilde{y} + \tilde{e}_0 + O(\epsilon), \dot{\tilde{y}} = \tilde{x}\tilde{y} \pm 1\}$ (we supposed that $\tilde{D} = \pm 1$). After the coordinate change $Y = -(\tilde{y} + \tilde{e}_0)$, and after division by $-1$, the vector field $X_S$, with $\epsilon = 0$, becomes: $\bar{X}_S : \{\dot{\tilde{x}} = Y, \dot{Y} = -\tilde{x}Y + (\pm 1 - \tilde{e}_0\tilde{x})\}$, where $\tilde{e}_0$ is kept in a compact set. This vector field is of the form (22) of [3], and therefore we can apply the results of Section 3.2.6 of [3]. Following Section 3.2.6 of [3] (Figures 3 and 4), the passage from $\tilde{x} = \infty$ to $\tilde{x} = -\infty$ in the family $\bar{X}_S$ is not possible. This implies that the passage from $\tilde{x} = -\infty$ to $\tilde{x} = +\infty$ in the family $X_S$ is not possible (we changed the time). Thus, the passage from the attracting branch to the repelling branch of the critical curve $\{\bar{y} = 0\}$ is not possible.

From now on, our focus will thus be on the chart $\{\tilde{e}_0 = 1\}$ of the sphere in the $(\tilde{D}, \tilde{e}_0, \tilde{e}_1)$-space.

2.3. **Difference map near $DF_{2a}$ and the divergence integral.** The limit cycles of $X_{\epsilon,b,(r^3\tilde{D},r^2,r\tilde{e}_1)}$ near $\cup_{x_*\in K}\Gamma_{x_*}$ can be studied as zeros of a difference map. We define a section $S_1 \subset \{x = 0\}$, parametrized by $x_* \in K$. More precisely, $S_1 = \{(0, \psi(x_*)) \mid x_* \in K\}$, where we suppose that the orbit of the system $\frac{1}{y}.X_{0,0,(r^3\tilde{D},r^2,r\tilde{e}_1)}$ through the point $(x_*, 0)$, $x_* \in K$, intersects the section $\{x = 0\}$ at a point denoted by $(0, \psi(x_*))$. Note that $\psi(x_*) > 1$ and $\psi'(x_*) > 0$ uniformly in $x_* \in K$. We define a second section $S_2 \subset \{\bar{X} = 0\} = \{x = O(\epsilon^2 D, \epsilon^2 e_0, \epsilon^2 e_1)\}$ parametrized by $\bar{Y} \sim 0$. Now if we follow the orbits of (4) in forward (resp. backward) time, we can define a transition map from $S_1$ to $S_2$ which we denote by $\Delta_+(x_*, \epsilon, r, \tilde{D}, \tilde{e}_1, b)$ (resp. $\Delta_-(x_*, \epsilon, r, \tilde{D}, \tilde{e}_1, b)$). See Figure 4. Closed orbits of (4) are given by zeros of the difference map

$$\Delta = \Delta_+ - \Delta_-.$$

**Lemma 2.1.** *The transition maps $\Delta_\pm$ can be written as*

$$\bar{Y} = \Delta_\pm(x_*, \epsilon, r, \tilde{D}, \tilde{e}_1, b) = -\epsilon^2 r^2 \tilde{\Delta}_\pm(x_*, \epsilon, r, \tilde{D}, \tilde{e}_1, b)$$

*where $\tilde{\Delta}_\pm$ are strictly positive $C^k$-functions in the variable $(x_*, \epsilon, r, \tilde{D}, \tilde{e}_1, b)$, with a $C^k$-extension to the boundary of their domain, and $\tilde{\Delta}_\pm(x_*, 0, r, 0, \tilde{e}_1, b) = 1$.*

*Proof.* Let's prove this for the transition map $\Delta_+$; the transition map $\Delta_-$ can be treated similarly. First we consider the transition map of $X_{\epsilon,b,(r^3\tilde{D},r^2,r\tilde{e}_1)}$ from the section $S_1$ to the section $\{\bar{X} = -\rho\}$, parametrized by $\bar{Y} \sim 0$, where $(\bar{X}, \bar{Y})$ are normal form coordinates and $\rho > 0$ is small. We denote this transition map by $\bar{Y} = \Delta_1(x_*, \epsilon, r, \tilde{D}, \tilde{e}_1, b)$ (see Figure 4). Following [1], the function $\Delta_1$ is smooth (smooth stands for $C^\infty$-smoothness) in $(x_*, \epsilon, r^3\tilde{D}, r^2, r\tilde{e}_1, b)$ with a smooth extension to the boundary $\{\epsilon = 0\}$ because the slow dynamics is regular along the attracting part of the critical curve. We define the second transition map of $X_{\epsilon,b,(r^3\tilde{D},r^2,r\tilde{e}_1)}$ from the section $\{\bar{X} = -\rho\}$, parametrized by the normal form coordinate $\bar{Y} \sim 0$, to the section $S_2$, denoted by $\bar{Y}_1 = \Delta_2(\bar{Y}, \epsilon, r, \tilde{D}, \tilde{e}_1, b)$. Note that $\Delta_2(\bar{Y}, \epsilon, r, \tilde{D}, \tilde{e}_1, b)$ also represents the transition map from the section $\{\bar{X} = -\rho\}$ to the section $S_2$ defined by following the orbits of (8), with $\tilde{e}_0 = 1$, in backward time, and by Theorem 2 of [3], it has the following form:

$$\bar{Y}_1 = \Delta_2(\bar{Y}, \epsilon, r, \tilde{D}, \tilde{e}_1, b) = -\epsilon^2 r^2 \bar{\Delta}_2(\bar{Y}, \epsilon, r, \tilde{D}, \tilde{e}_1, B_0, B_2, b) \tag{9}$$

where $\bar{\Delta}_2$ is a strictly positive $C^k$-function on the topological closure of its domain. Moreover, Theorem 1 of [3] implies that

$$\bar{\Delta}_2(\bar{Y}, 0, r, \tilde{D}, \tilde{e}_1, 0, B_2, b) = 1. \tag{10}$$

Clearly, the transition map $\Delta_2$ is a local $C^k$-diffeomorphism with respect to $\bar{Y}$ whenever it exists. Although the transition map does not exist when $\epsilon = 0$, the function $\bar{\Delta}_2$, introduced in (9), can be $C^k$-extended to the boundary $\epsilon = 0$ where we obtain (10).

We now combine (9) with the fact that

$$\Delta_+(x_*, \epsilon, r, \tilde{D}, \tilde{e}_1, b) = \Delta_2(\Delta_1(x_*, \epsilon, r, \tilde{D}, \tilde{e}_1, b), \epsilon, r, \tilde{D}, \tilde{e}_1, b),$$

to obtain the above result for the transition map $\Delta_+$. □

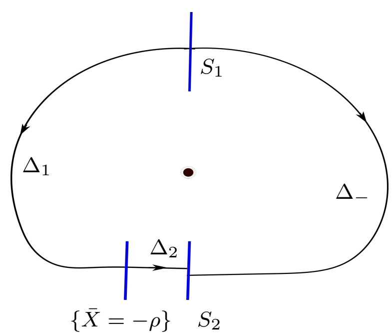


FIGURE 4. The transition maps $\Delta_+ = \Delta_2 \circ \Delta_1$ and $\Delta_-$.

The following proposition (see [1]) allows us to express the derivative of the difference map $\Delta$ w.r.t. $x_*$ in terms of a divergence integral.

**Proposition 1** ([1]). *Let $f$ be a vector field on an open subset of $\mathbb{R}^n$. Let $S_1$ and $S_2$ be two open sections of $\mathbb{R}^n$, transverse to the flow of $f$. Assume $p \in S_1$, $q \in S_2$ and the orbit through $p$ reaches $q$ in finite time. Let $T : S_0 \subset S_1 \to S_2$ be the transition map defined in a neighborhood of $p$. If $\phi_i : U_i \to S_i$ are coordinates for $S_i$ with $U_i \subset \mathbb{R}^{n-1}$, then*

$$\det(D(\phi_2^{-1} \circ T \circ \phi_1))(s_1) = \frac{\det(D\phi_1(s_1)|f(p))}{\det(D\phi_2(s_2)|f(q))} \exp\left\{ \int_{O(p,q)} \operatorname{div} f \, dt \right\},$$

*where $s_1 = \phi_1^{-1}(p)$, $s_2 = \phi_2^{-1}(q)$, and where $(D\phi_1(s_1)|f(p))$ is a matrix composed of the $n \times (n-1)$ matrix $D\phi_1(s_1)$ and the column vector $f(p)$, and similarly for $(D\phi_2(s_2)|f(q))$. The integral is taken over the orbit $O(p,q)$ from $p$ to $q$ parametrized by $t$.*

Using Proposition 1, the fact that $S_2 \subset \{x = O(\epsilon^2 r^3 \widetilde{D}, \epsilon^2 r^2, \epsilon^2 r \tilde{e}_1)\}$ and

$$\bar{Y} = -\frac{y(1 + bx - y) + \epsilon^2(r^2 + r\tilde{e}_1 x + x^2)}{1 + O(\epsilon)}, \tag{11}$$

we have that

$$\frac{\partial \tilde{\Delta}_\pm}{\partial x_*} = \frac{-L(x_*, \epsilon, D, e_0, e_1, b)}{\epsilon^4 r^4 \tilde{\Delta}_\pm} \exp\left(\mathcal{I}_\pm(x_*, \epsilon, D, e_0, e_1, b)\right)$$

where $(D, e_0, e_1) = (r^3\tilde{D}, r^2, r\tilde{e}_1)$, $L$ is a strictly positive smooth function, and with

$$\mathcal{I}_\pm(x_*, \epsilon, D, e_0, e_1, b) = \int_{\mathcal{O}^\pm(x_*,\epsilon,D,e_0,e_1,b)} \text{div } (\pm X_{\epsilon,b,(D,e_0,e_1)})dt$$

where $\mathcal{O}^+(x_*, \epsilon, D, e_0, e_1, b)$ (resp. $\mathcal{O}^-(x_*, \epsilon, D, e_0, e_1, b)$) is the orbit of the system $X_{\epsilon,b,(D,e_0,e_1)}$ through the point $(0, \psi(x_*)) \in S_1$, in positive time (resp. in negative time) until it hits the section $S_2$. If we denote the divergence integral $\mathcal{I}_+ - \mathcal{I}_-$ by $\mathcal{I}$, and if we define the positive analytic function $E(\alpha_1, \alpha_2) = \frac{\exp\alpha_1 - \exp\alpha_2}{\alpha_1 - \alpha_2}$, $\alpha_1 \neq \alpha_2$, and $E(\alpha_1, \alpha_2) = \exp\alpha_1$, then we obtain

$$\frac{\partial\Delta}{\partial x_*} = -\epsilon^2 r^2 \frac{\partial(\tilde{\Delta}_+ - \tilde{\Delta}_-)}{\partial x_*} = \frac{L}{\epsilon^4 r^2} E(\alpha_1, \alpha_2)\Big(\epsilon^2\mathcal{I} + \epsilon^2 \ln\frac{\tilde{\Delta}_-}{\tilde{\Delta}_+}\Big) \tag{12}$$

where

$$\alpha_1 = \mathcal{I}_+ - \ln\tilde{\Delta}_+, \ \ \alpha_2 = \mathcal{I}_- - \ln\tilde{\Delta}_-.$$

The derivative of $\epsilon^2\mathcal{I} + \epsilon^2 \ln\frac{\tilde{\Delta}_-}{\tilde{\Delta}_+}$ in (12) is given by

$$\epsilon^2 \frac{\partial\mathcal{I}}{\partial x_*} + \epsilon^2\Big(\frac{\frac{\partial\tilde{\Delta}_-}{\partial x_*}}{\tilde{\Delta}_-} - \frac{\frac{\partial\tilde{\Delta}_+}{\partial x_*}}{\tilde{\Delta}_+}\Big). \tag{13}$$

The reason we study the derivative (13) is twofold: it is that the function $\epsilon^2 \frac{\partial\mathcal{I}}{\partial x_*}(x_*, \epsilon, D, e_0, e_1, b)$ is $C^k$ on the topological closure of its domain, and

$$\epsilon^2 \frac{\partial\mathcal{I}}{\partial x_*}(x_*, \epsilon, D, e_0, e_1, b)\big|_{\epsilon=0} = \frac{\partial I}{\partial x_*}(x_*, b, e_0, e_1),$$

where $\frac{\partial I}{\partial x_*}$ is given in (3) (see Theorem 4 and Section 4.2 of [3]), and the other reason is that

**Lemma 2.2.** *The functions* $\frac{\partial\tilde{\Delta}_\pm}{\partial x_*}$ *and* $\frac{\frac{\partial\tilde{\Delta}_\pm}{\partial x_*}}{\tilde{\Delta}_\pm}$ *are* $C^k$*-functions w.r.t. original variable* $(x_*, \epsilon, D, e_0, e_1, b)$ *on the closure of their domain.*

*Proof.* We focus on $\frac{\partial\tilde{\Delta}_+}{\partial x_*}$ and $\frac{\frac{\partial\tilde{\Delta}_+}{\partial x_*}}{\tilde{\Delta}_+}$ ($\frac{\partial\tilde{\Delta}_-}{\partial x_*}$ and $\frac{\frac{\partial\tilde{\Delta}_-}{\partial x_*}}{\tilde{\Delta}_-}$ can be treated similarly). We have

$$\frac{\partial\tilde{\Delta}_+}{\partial x_*} = \frac{\partial\bar{\Delta}_2}{\partial\bar{Y}}(\Delta_1(\dots), \dots).\frac{\partial\Delta_1}{\partial x_*}(\dots)$$

and

$$\frac{\frac{\partial\tilde{\Delta}_+}{\partial x_*}}{\tilde{\Delta}_+} = \frac{\frac{\partial\bar{\Delta}_2}{\partial\bar{Y}}}{\bar{\Delta}_2}(\Delta_1(\dots), \dots).\frac{\partial\Delta_1}{\partial x_*}(\dots),$$

where $\Delta_1$ and $\bar{\Delta}_2$ are defined above. Following [1], $\Delta_1$ and $\frac{\partial\Delta_1}{\partial x_*}$ are smooth functions w.r.t. $(x_*, \epsilon, D, e_0, e_1, b)$ on the topological closure of their domain, hence including $\{\epsilon = 0\}$. From (7) and Theorem 3 of [3], the functions $\frac{\partial\bar{\Delta}_2}{\partial\bar{Y}}$ and $\frac{\frac{\partial\bar{\Delta}_2}{\partial\bar{Y}}}{\bar{\Delta}_2}$ are $C^k$ w.r.t. $(\bar{Y}, \epsilon, b_0, b_1, b_2, D, e_0, e_1, b)$ on the topological closure of their domain, and are hence $C^k$ w.r.t. $(\bar{Y}, \epsilon, D, e_0, e_1, b)$. This concludes the proof of the lemma. □

Let's write $F(x_*, b) = F_b(x_*)$. Proposition 4.1 of [5] implies that

$$\frac{\partial F}{\partial b}(x_*, 0) = -1 + \frac{x_*^2 + 1}{x_*}\arctan x_* - \pi\frac{x_*^2 + 1}{x_*}, \ F(x_*, 0) = -x_*. \tag{14}$$

Using (3) and (14), $\frac{\partial I}{\partial x_*}(x_*, b, e_0, e_1)$ can be written as

$$e_1\Big(-\frac{2}{x_*^2}+O(e_0,e_1,b)\Big)+b\Big(2\frac{1-\frac{\arctan x_*}{x_*}+\frac{\pi}{x_*}}{x_*^2}+O(e_0,e_1,b)\Big). \quad (15)$$

Since $B_0$ in (8) is a "breaking parameter" (see [3] or [7]), periodic orbits of systems $X_{\epsilon,b,(r^3\tilde{D},r^2,r\tilde{e}_1)}$, Hausdorff-close to $\Gamma_{x_*}$, can exist only for $\tilde{D}=\tilde{D}_0(x_*,\epsilon,r,\tilde{e}_1,b)$ where $\tilde{D}_0(x_*,\epsilon,r,\tilde{e}_1,b)$ is a $C^k$-function. This follows directly from the Implicit Function Theorem because $B_0=\tilde{D}+O(\epsilon)$, $(\tilde{\Delta}_+-\tilde{\Delta}_-)(x_*,0,r,0,\tilde{e}_1,b)=0$ and $\frac{\partial(\tilde{\Delta}_+-\tilde{\Delta}_-)}{\partial\tilde{D}}(x_*,0,r,0,\tilde{e}_1,b)\neq 0$. Furthermore, since $X_{\epsilon,b,(r^3\tilde{D},r^2,r\tilde{e}_1)}$ has a center for $(\tilde{D},\tilde{e}_1,b)=(0,0,0)$, we have

$$\Delta(x_*,\epsilon,r,0,0,0)=0$$

and

$$\tilde{D}_0(x_*,\epsilon,r,0,0)=0.$$

Since (15) is identically zero for $b=e_1=0$, it is more convenient to study zeros w.r.t. $x_*$ of

$$\Delta_p(x_*,\epsilon,r,\tilde{e}_1,b)=\Delta(x_*,\epsilon,r,\tilde{D}_0(p,\epsilon,r,\tilde{e}_1,b),\tilde{e}_1,b)$$

where $p$ is kept in the compact set $K$. We call this procedure "cloning a variable" (see [7]). Note that $\frac{\partial\Delta_p}{\partial x_*}(x_*,\epsilon,r,0,0)=0$. If we now substitute in (12) the function $\tilde{D}_0(x_*,\epsilon,r,\tilde{e}_1,b)$ for $\tilde{D}$, and use (15) and the fact that the function in (13) is $C^k$ w.r.t. to the original parameters $(D,e_0,e_1)$, then (13) can be written as

$$e_1\Big(-\frac{2}{x_*^2}+O_1(\epsilon,e_1,b)\Big)+b\Big(2\frac{1-\frac{\arctan x_*}{x_*}+\frac{\pi}{x_*}}{x_*^2}+O_2(\epsilon,e_1,b)\Big) \quad (16)$$

where $O_1$ and $O_2$ are $C^k$-functions w.r.t. $(x_*,\epsilon,r,\tilde{e}_1,b,p)$. In the rest of this section we will show that (16) has at most 1 zero (counting multiplicity) w.r.t. $x_*\in K$, with $(e_1,b)\neq(0,0)$. Using (12) and Rolle's theorem, this will imply that the difference map $\Delta$ has at most 3 zeros (counting multiplicity) w.r.t. $x_*\in K$ for $\epsilon>0$, $r>0$ and $(\widetilde{D},\widetilde{e}_1,b)\neq(0,0,0)$, which will conclude the proof of Theorem 1.1.

If we define rescaling $(e_1,b)=(\kappa\bar{e}_1,\kappa\bar{b})$, $(\bar{e}_1,\bar{b})\in\mathbb{S}^1$, $\kappa\sim 0$, $\kappa\geq 0$, then expression (16) can be written as

$$\frac{2}{x_*^2}\kappa\Big(-\bar{e}_1+\bar{b}\big(1-\frac{\arctan x_*}{x_*}+\frac{\pi}{x_*}\big)+O(\epsilon,\kappa)\Big) \quad (17)$$

where $x_*\in K$. This rescaling is the so-called Bautin trick.

When $\kappa=0$, we deal with a center. Thus we suppose that $\kappa>0$. We will show that the expression

$$-\bar{e}_1+\bar{b}\big(1-\frac{\arctan x_*}{x_*}+\frac{\pi}{x_*}\big) \quad (18)$$

has at most 1 zero (counting multipicity) with respect to $x_*\in K$, for each $(\bar{e}_1,\bar{b})\in\mathbb{S}^1$. This will imply that the expression in (17) has at most 1 zero counting multiplicity in $K$ for each $(\bar{e}_1,\bar{b})\in\mathbb{S}^1$, $\kappa>0$, $\kappa\sim 0$ and $\epsilon\sim 0$.

When $(\bar{e}_1,\bar{b})=(\pm 1,0)$, the expression (18) has no zeros in $K$. When $(\bar{e}_1,\bar{b})\in\mathbb{S}^1$ and $\bar{b}\neq 0$, we consider the derivative of (18):

$$-\frac{\bar{b}}{x_*^2(1+x_*^2)}\big(x_*-(1+x_*^2)\arctan x_*+\pi(1+x_*^2)\big). \quad (19)$$

If we write $l(x_*) = x_* - (1 + x_*^2)\arctan x_* + \pi(1 + x_*^2)$, then we have that $l(0) = \pi$ and

$$l'(x_*) = 2x_*(\pi - \arctan x_*) > 0$$

for all $x_* > 0$. Thus we have that $l(x_*) > 0$ for all $x_* \in K$. This implies that (19) has no zeros in $K$ and, by Rolle's theorem, (18) has at most 1 zero counting multiplicity in $K$. This completes the proof of Theorem 1.1.

## REFERENCES


[1] P. De Maesschalck and F. Dumortier, Time analysis and entry-exit relation near planar turning points, *J. Differential Equations*, **215** (2005), 225–267.

[2] P. De Maesschalck and F. Dumortier, Canard cycles in the presence of slow dynamics with singularities, *Proc. Roy. Soc. Edinburgh Sect. A*, **138** (2008), 265–299.

[3] P. De Maesschalck and F. Dumortier, Singular perturbations and vanishing passage through a turning point, *J. Differential Equations*, **248** (2010), 2294–2328.

[4] F. Dumortier and R. Roussarie, Canard cycles and center manifolds, *Mem. Amer. Math. Soc.*, **121** (1996), x+100.

[5] F. Dumortier and C. Rousseau, Study of the cyclicity of some degenerate graphics inside quadratic systems, *Commun. Pure Appl. Anal.*, **8** (2009), 1133–1157.

[6] F. Dumortier, R. Roussarie and C. Rousseau, Hilbert's 16th problem for quadratic vector fields, *J. Differential Equations*, **110** (1994), 86–133.

[7] R. Huzak, P. De Maesschalck and F. Dumortier, Limit cycles in slow-fast codimension 3 saddle and elliptic bifurcations, *J. Differential Equations*, **255** (2013), 4012–4051.

[8] C. Rousseau, Normal forms, bifurcations and finiteness properties of vector fields, in *Normal forms, bifurcations and finiteness problems in differential equations, volume 137 of NATO Sci. Ser. II Math. Phys. Chem.*, Kluwer Acad. Publ., Dordrecht, (2004), 431–470.

[9] S. Smale, Mathematical problems for the next century, in *Mathematics: frontiers and perspectives*, Amer. Math. Soc., Providence, RI, (2000), 271–294.